A Crowd-Sensing System for Geomatics Applications

Lorenzo Boccia[1], Alessandra Capolupo[2(✉)], Giuseppina Esposito[1], Giuseppe Mansueto[1], and Eufemia Tarantino[3]

[1] Department of Architecture, University of Naples Federico II, Via Forno Vecchio, 12, 80134 Naples (NA), Italy
[2] Plinivs Research Center - LUPT, University of Naples Federico II, Via Toledo, 402, 80134 Naples (NA), Italy
alessandra.capolupo@unina.it
[3] DICATECh, Politecnico di Bari, Via E. Orabona 4, 70125 Bari, Italy

Abstract. Risk prevention is recognized as one of the most critical aspects of the policies of environmental monitoring. Because of the limited resources and the large amount of structures used for erosion control and slope protection, the Civil Protection and the Italian Forestry Carabinieri are not able to supervise them directly, with enough frequency. The present work is aimed to develop an innovative technique for periodically monitoring those structures, combining Mobile Crowd-Sensing (MCS) technology with photogrammetry and GIS. The experiments were performed in the Nature Reserve of Tirone (a protected natural area located inside the Vesuvius National Park in Naples) by analysing the metric reconstruction of two structures (a small weir and a log crib wall), before and after an accident, artificially generated for simulating a hydrogeological event or an act of vandalism, in order to evaluate GCPs influence. The procedure was split into four main phases: periodic acquisition of sets of photos with common smartphones and their transmission via the Internet; elaboration of the threedimensional model starting from a subset of selected pictures; comparison between the generated and the previous model; database update and programming of the subsequent monitoring. The accuracy of photogrammetric reconstructions was evaluated comparing the reconstruction with and without Ground Control Points (GCPs). The results show the models extracted without GCPs are satisfactory, since they allow to retrieve dimensional information of the examined constructions and to detect any instability. Models, generated using GCPs, are more detailed, but the processing and operational time is strongly higher.

Keywords: Crowd sensing · Photogrammetry · Structures monitoring

1 Introduction

The Italian Statistical Institute (ISTAT) classifies the national territory into 35.2% of mountains, 41.6% of hills and only 23.2% of plains. In such a morphologically complex territory, a large hydrogeological instability ensues [1]. Disastrous events such 2 as ones occurred in Liguria Region in 2011 and 2014, in Messina and Giampilieri in 2009, in Sarno in 1998, in Amalfi coast in 1954, causing more than 500 life losses and

© Springer Nature Switzerland AG 2019
S. Misra et al. (Eds.): ICCSA 2019, LNCS 11622, pp. 297–312, 2019.
https://doi.org/10.1007/978-3-030-24305-0_23

huge damages to the built environment. [2] expressed the Risk (R) as the convolution of Hazard intensity (H), Exposure (E) and vulnerability (V) (Eq. 1):

$$R = H * E * V \tag{1}$$

Currently, risk assessment and management is an essential operational field to tackle and monitor hydrological instability, even if a promising result may be achieved only thanks to a permanent and constant activity. All of this implies that the permanent management of the mountain and hill territory, where are a large amount of structures used for the erosion control or slope stabilization, built using both traditional techniques and bioengineering approaches, is necessary in addition to the management of watercourses and the main landuse. Some small structures, such as small weirs, retaining walls, live fascines, brush layering and palisades, small stream diversions etc., are individually characterized by a little importance; on the contrary, when they are grouped and considered together, they represent fundamental elements able to protect the territory. An inventory plan of these constructions, commonly built without a real project and not subjected to any maintained plan, is missed and, therefore, often, they are not subjected to any monitoring by Basin Authorities, Regions and Civil Protection. Moreover, many of them are also located in areas difficult to access and to notice. These situations exceeds 10000 units, although our estimate exceeds 50000 situations on the Italian national territory. In the past, the State Forestry Corps, a police force responsible for governing and controlling the agro-forestry area, now called Carabinieri Forestali, exercise a monitoring and control action. The use of the mountains and hills for agro-livestock activities was itself a monitoring action. Because of the progressive urbanization, the reduction of the Carabinieri Forestry and the new assigned tasks, the problem of technical monitoring becomes even more important. In the forestry field, the satellite imagery and/or drone technology has not brought the same advantages as in other areas due to the presence of vegetation. Monitoring have to be carried out by explorers. Furthermore, monitoring is qualitative and the decision-making action in the event of changes in the state of the places belongs to the explorers. The scout must have a considerable technical skill and know the single construction. The interest in modern monitoring, on the contrary, is focused in reducing the operational time and the involvement of technicians, leaving them the ultimate choice and the ultimate responsibilities but not the operational tasks, assigned to less qualified staff. Not a high accuracy is required for those kind of structures, therefore that metric reconstruction should be satisfactory. Nowadays, the awareness of citizens is more sensitive and open-minded regarding the environment and the protection of the territory; moreover, many of them are also available to share information and data (Crowd). In the meanwhile, new methodolo- 3 gies are available, such as smartphones equipped with high resolution cameras and a built-in Global Position System (GPS). Also the 4G network, available since 2013 in most of the nations, is an essential prerequisite to largely widespread the smartphone use in surveying. The latest generation photogrammetry is undoubtedly much faster than in the past and authors such as [3–6] try urban buildings and artifact reconstructions, without ground control points.

According to these premises the research is aimed to demonstrate the possibility to create an integrated technology, suitable for delegating to surveyors not nspecialized,

the scout action. Evaluating how to obtain an elaboration suitable to emphasize any critical issues and reduce the intervention of the high profile technicians only during the decision-making moment, on the basis of sufficiently detailed and sufficiently accurate quantitative information, is in additional purpose of the current research activity. The high skilled technician, thanks to this support, should be able to take a binary decision regarding the monitoring rescheduling or related the necessary to send a specialized engineer on the field to supervise the structures [7].

2 Materials and Method

2.1 Study Area and Selection of the Structures to Be Investigated

The experiment was conducted in Tirone-Alto Vesuvio Reserve, in the area of the Vesuvius National Park in the Province of Naples (southern Italy), characterized by the presence of small hydraulic-forestry structures, built using both traditional techniques and naturalistic engineering techniques. During a first survey, two study cases, representing a widespread constructions typology in the Campania Region that can be investigated by applying the crowd sensing, were selected: a log crib wall and a small weir. More than 2000 of these structures are scattered throughout Campania Region [8].



Fig. 1. Study case in the Tirone Alto-Vesuvio Reserve (Vesuvius Natural Park. Napoli, Italy): (a) structure 2 - log crib wall, (b) structure 5 – small weir to prevent gulling and land sliding in a occasional stream.

The former (Fig. 1a) is a grid of wooden trunks (a log crib wall), able to support a small slope of about 5 m and about 15 m in height and in plan, respectively. The frequency of its maintenance is typically fixed to ten-years. The latter (Fig. 1b) is a small weir (properly a step) long about 5 m and height about 1.50 m. The outflanking due to stream diversions, the breaking of the crest and the sediment accumulation upstream are the typical failures of these constructions. Verifying both the maintenance status and the functionality of the construction is the final purpose.

2.2 Operational Workflow

All the applied procedure is summarized in the workflow, described in Fig. 2. It consists of five steps:

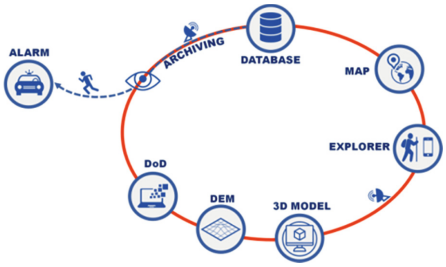

Fig. 2. Proposed workflow

1. creating a digital database (DB) of the structures of the territory to be monitored;
2. generating maps of georeferenced flags;
3. surveying the camp by applying selected operators or volunteers, called by us "scout";
4. Carrying out photogrammetric and GIS elaboration through specialized operators (3D model, DEM, DoD);
5. evaluating the risk: reporting alarm and/or updating of database.

The database (DB) has to be developed on an online platform and progressively updated and integrated with new information and objects. The complete geographic information has to be collected and organized for each structure. The DB must report the date of last inspection and that one of subsequent survey, the authorized scouts, risk level classification, the historical series of acquired image sets, photogrammetric reconstructions, DEM etc. The database produces periodically a set of viewpoints (flags), that will be sent to a group of scouts. Each scout receives all the information related to the target that he should survey.

The scout acquires the images of the target by applying an own Smartphone. In our case, we used a Smartphone, an Iphone 7 Plus. The scout has to follow the specific 5 guidelines with the support of a certified App and tutorials. The surveys must be carried out during the day, possibly avoiding time slots in which shadows are too sharp. The device must be keep vertical with the A-GPS turned on. Collecting an adequate number of images, characterized by the overlap of 60% and 80%, longitudinally and transversally direction, respectively, in order to assure that every point appears in three images at least [9]. In perspective, a dedicated App will implement various functions, like as the zoom block, the vibrations for the nonverticality of the sensor, the real time check of defocused and blurry images, and the measure of the distance between camera positions. SfM (Structure from Motion) software's is necessary to collect the images during the movement [10]. When the images of the target are acquired by a camera, the app should also inform the scout, though an acoustic signals, if its motion is too fast [11].

Subsequently, the acquired data will be sent via 4G or Wi-fi to a powerful calculation station. Photogrammetric elaboration will be performed by a specialist with a dedicated photogrammetric software. The procedure was described in depth in [12, 13]. Once the virtual inspection of the metric reconstruction and the measure of any defect points have been completed, any degradation situations and the estimation of the accumulated materials will be investigated through the comparison between the baseline and the successive 3D models.

The 3D model will be obtained thanks to through the metric reconstruction. The outcome of this step is the generation of a high resolution Digital Elevation Model (DEM). The comparison between the two DEMs, overlapping them, highlights all the dimensional anomalies and allows to quantify the differences. The outcome of that procedure is the Dem of Differences (DoD) [14]. This operation is pretty laborious since the models generated by the photogrammetric reconstructions without (GCPs Ground Control Points) cannot be geo-located with sub-metric precision, and, therefore, the DEMs reposition should be performed. This step allows to emphasize and objectively quantify some issues, such as an excessive deposition, erosion of weir material, undercutting, debris upstream or downstream of a weir, etc. The final step is related to the evaluation of the operation capability of the specialist to identify and quantify the action need without using instrumental measures. Just few technicians are skilled for such kind of decisions. These skilled technicians are involved only in this phase. Their decision will be supported by the 3D models and the DoD. In any case, all acquired and processed images are archived into the database in view of the next monitoring campaign. The alarming situations are signalled and checked with inspections and interventions or notifications.

2.3 Crowd Sensing Operations

For each case study, about 100 photographs were taken using a iPhone7 Plus, equipped with a 12 MP wide-angle camera - pixel size of 1.22 microns and a focal length of 3.99 mm. At a shooting distance shorter than 15 m, the Ground Sample 6 Distance (GSD) is better than 5 mm. The autofocus zoom effect and all pre-calibrated settings were deactivated. The operator, moving himself sideways with single steps from a short distance (5-8 m), acquired three sets of about 30 photos: the former keeping the camera at chest height (1.2 m), the latter at eye level (1.7 m) and, the last slightly inclining the camera (tilt of about 15°) at the height of about 2 m (Fig. 3). On the second site, a damage or a vandalism act was simulated. The purpose is to validate the methodology in case of changes in the state of a forestry structure (Fig. 4). 3D model reconstructions of each structure, were obtained with the software Agisoft PhotoScan. The initial step is the alignment of the input photos. The algorithms of PhotoScan automatically identify the tie points in each photo and build the Sparse Points Cloud and realign the photos. Really, since the GCPs coordinates are in ETRS 89, when these GCPs are used, the photos are reoriented in ETRS 89 ETRF2000. The GCPs, if used, were localized manually in each photos (Figs. 5, 6 and 7 and Tables 1 and 2).

In order to assess the accuracy of the photogrammetric reconstructions, a series of paper targets (black and white circle of 80 mm in diameter) were positioned along the areas of interest and their coordinates were measured. The survey of Ground Control

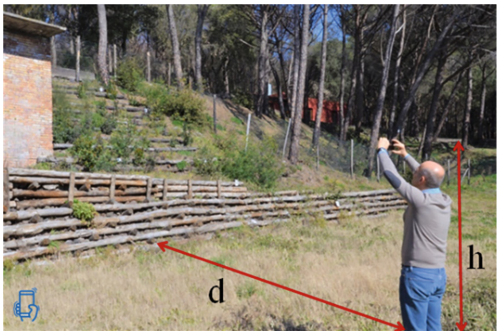

Fig. 3. Example of image acquisition: H is the height of camera sensor and d is the distance between the operator and the structure 2.



Fig. 4. Simulated damage in front to Structure 5.



Fig. 5. Three-dimensional reconstruction of Structure 2 with the GCPs



Fig. 6. Three-dimensional reconstruction of Structure 5 with the picture alignment

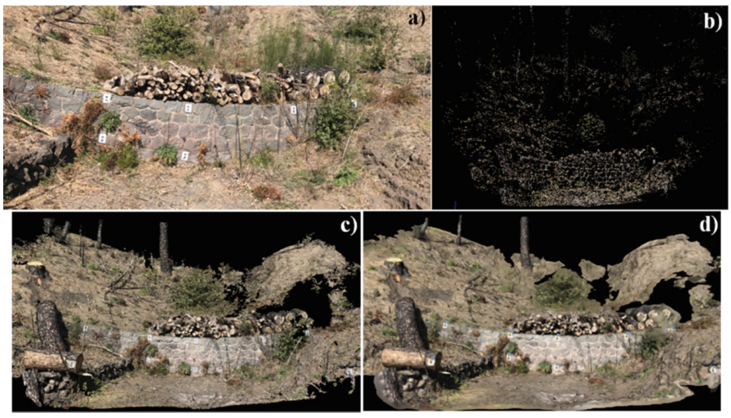

Fig. 7. Workflow reconstruction of structure 5: (a) Loading Photos with target, (b) Reconstruction of a Sparse Point Cloud, (c) Reconstruction of Dense Point Cloud, (d) Build 3D Mesh (the GCPs are blue flags and in this case are used only for dimensional control of the results) (Color figure online)

Table 1. Number of points elaborated for a three-dimensional reconstruction

Structure 2	No. of photos	Sparse points	Dense points
With GCPs	38	2.6×10^4	1.2×10^6
Without GCPs	38	2.3×10^4	1.2×10^6

Table 2. Number of points elaborated for a three-dimensional reconstruction

Structure 5	No. of photos	Sparse points	Dense points	DEM resolution (mm/pixel)
With GCPs	42	2.4×10^4	1.2×10^7	3.96
Without GCPs	40	2.5×10^4	1.2×10^7	4.88
Without GCPs	48	2.3×10^4	1.4×10^7	4.43

Points (GCPs) was carried out using a Geomax GPS Zenith 35, connected via 4G to the Campania Region's permanent network of stations to obtain, in real time, the signal corrections (Differential Global Positioning System in RTK DGPS). In forestry field, this DGPS configuration is susceptible to reflections and disturbance to GPS signal (due to weak 4G connection, presence of tall vegetation), so it was decided to use also a Geodimeter 600 PRO total station. Since it was desired to obtain coordinates of the GCPs in ETRS89 ETRF 2000 system, the surveys, carried out using the total station, were calculated by orienting the station applying the inverse intersection (Snellius Pothenot), manually solved on three DGPS points, using points where the GPS had provided good accuracies. Furthermore, it was decided to compare photogrammetric 3D reconstruction with and without GCPs for each site. As suggested by [15] the accuracy was evaluated by computing the scatterplot between the measured and the estimated values (Fig. 8).



Fig. 8. (a) Target, (b) Measurement of the GCPs by Structure 2 using DGPS, (c) Measurement of the coordinates of GCPs by Structure 5 using dGPS, (d) Measurement of GCPs by Structure 2 with the Total Station

3 Results

In order to evaluate the reconstruction accuracy, 13 mutual Euclidian distances among the GCPs coordinates were calculated. Subsequently, in each reconstruction with GCPs, the same distances were measured with the "Scale Bar" tool of the Software Agisoft: the paper target were directly detected on the 3D model and a yellow line joined the selected points. Figure 9 shows the decimated mesh of structure 2: the scale bars in part A were more accurate than the scale bars of the part B.

The two reconstructions without GCPs and targets were opportunely scaled using one reference distance as input, in order to obtain the same effect that is possible inserting in the photo scene a Range Pole. For the first structure, the reference distance is 1.46 m between the GCPs 1003 and 1004, and for the second structure is 1.40 m between GCPs 2018–2020. After this operation, a new mesh was created and the

distances (reported in the table) were measured. Figure 10 shows the same reference scale bar in two pictures, one with targets and the other without them. In the second case, the recognition of the reference points is more difficult. Figure 10c shows the scale bars obtained for the second structure after the simulated damage. After the simulated damage, the point 2021 was covered by the woods and, in this case, was impossible to measure the Euclidean distances. The results of measurements and their comparison in term of difference and percentage difference were listed in Tables 3, 4, 5, 6 and 7. Moreover, in order to evaluate outcomes accuracy also the average (μ), the Root Mean Square Error (RMSE) (Tables 3, 4, 5 and 6), scatterplots and coefficient of correlation (Fig. 11).

The best results were obtained from the model reconstruction with the aid of GCPs, with a standard deviation of 0.02 for the first structure and 0.04 for the second structure. As expected, the standard deviations of the differences obtained from the comparison with the reconstructions without GCPs and the Euclidean distances are highest (0.13 for the structure 2 and 0.09 for the structure 5). The distance measured on the 3D model of the structure 5 after the damage compared with the Euclidian distance gives an excellent result in term of standard deviation ($\sigma = 0.05$). These results demonstrate that the methodology is consistent with the aim of the paper. For these structures, actually commonly monitored without any measure but only on the base of the experience, an accuracy of the order of 0.1 m is largely satisfactory. The scatterplot and the coefficient of correlation of each group composed by estimated and measured points show a very high values: R^2 is higher than 0.99.

The Digital Elevation Models (DEMs) of the site 5 - before and after damage - were generated in Agisoft PhotoScan. The first and the second DEMs was georeferenced using ArcMap and overlap. DEMs are shown in Figs. 11 and 12. The colour scale ranges from red (inferior altitude) to green (superior altitude). The DoD was generated by subtracting the DEM before and after the damage. Figure 13 illustrates the DoD: the red areas represent the negative differences in altitude and the yellow areas indicates the

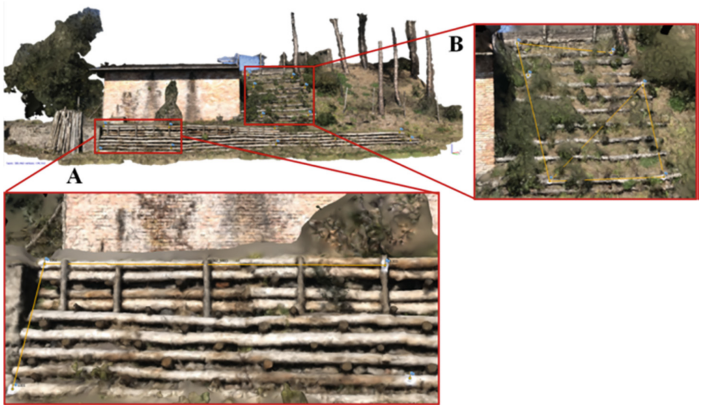

Fig. 9. Zoom of the 3D model of the Structure 2: (A) (B). Detail of the scale bar used to measure and the distance between three GCPs (1001. 1002. 1003) for the comparison with the measures with the total station.



Fig. 10. Scale Bar between GCPs 2018 and 2020 of Structure 5 in (a) photo with Target, (b) photo without Target, (c) 3D Model post-damage.

positive difference. The blue areas reflect the absence of surface reconstruction. The areas in green are characterized by negligible differences in terms of altitude. The DoD emphasizes the failure when submitted to the attention of an expert of the forestry service.

Table 3. Euclidean distance between point A and point B of structure 2, calculated using the coordinates: measured (second column) and estimated from the reconstruction of the 3D model with Target Ground Control Points (third column). Difference between measured distance and the estimated distance (fourth column) and percentage difference (fifth column). SD: Standard Deviation, μ: average, RMSE: Root Mean Square Error

ID point	Measured distance (m)	Measured distance with GCPs (m)	Difference (m)	Percentage difference (%)
1001–1002	1.84	1.85	0.008	0.43
1001–1003	5.05	5.02	−0.023	0.46
1001–1004	5.01	5.00	−0.018	0.37
1001–1005	12.17	12.15	−0.015	0.12
1001–1006	12.13	12.12	−0.019	0.16
1002–1003	4.81	4.79	−0.018	0.37
1007–1008	4.33	4.27	−0.060	1.39
1008–1009	0.84	0.84	0.00004	0.005
1010–1011	3.70	3.70	−0.001	0.02
1010–1012	6.34	6.33	−0.006	0.10
1010–1014	7.87	7.89	0.021	0.27
1011–1012	4.98	4.98	−0.004	0.07
1014–1015	4.22	4.21	−0.007	0.16
SD			**0.02**	
μ			**0.01**	
RMSE			**0.02**	

Table 4. Euclidean distance between point A and point B of structure 2, calculated using the coordinates: measured (second column) and estimated from the reconstruction of the 3D model without Target Ground Control Points (third column). Difference between the measured distance and the estimated distance (fourth column) and percentage difference (fifth column). SD: Standard Deviation, μ: average, RMSE: Root Mean Square Error

ID point	Measured distance (m)	Measured distance without GCPs (m)	Difference (m)	Percentage difference (%)
1001–1002	1.84	1.78	0.057	3.12
1001–1003	5.05	4.88	0.163	3.24
1001–1004	5.01	4.82	0.191	3.81
1001–1005	12.17	11.72	0.447	3.67
1001–1006	12.13	11.74	0.389	3.21
1002–1003	4.81	4.65	0.154	3.20
1007–1008	4.33	4.21	0.117	2.70
1008–1009	0.84	0.82	0.028	3.32
1010–1011	3.70	3.60	0.098	2.64
1010–1012	6.34	6.08	0.257	4.05
1010–1014	7.87	7.47	0.396	5.03
1011–1012	4.98	4.80	0.183	3.68
1014–1015	4.22	3.99	0.232	5.51
SD			**0.13**	
μ			**0.01**	
RMSE			**0.02**	

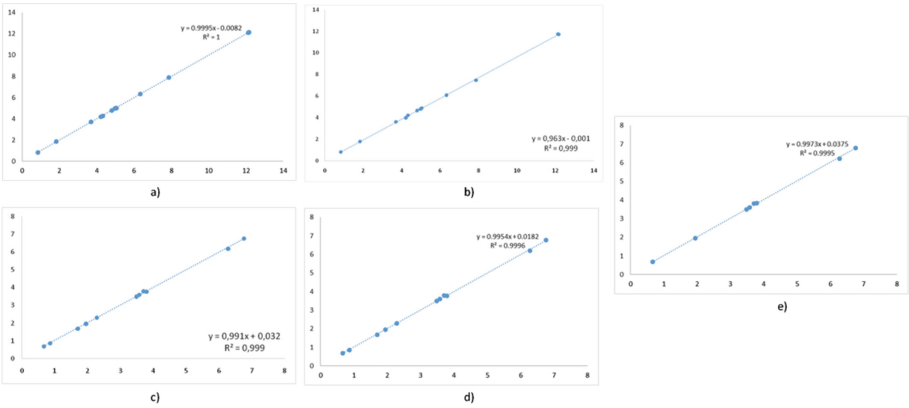

Fig. 11. Scatterplot between measured and estimated values. (a) Scatterplot corresponding to Table 3, (b) Scatterplot corresponding to Table 4, (c) Scatterplot corresponding to Table 5, (d) Scatterplot corresponding to Table 6, (e) Scatterplot corresponding to Table 7.

Table 5. - Euclidean distance between point A and point B of structure 5, calculated using the coordinates: measured (second column) and estimated from the reconstruction of the 3D model with Target Ground Control Points (third column). Difference between the measured distance and the estimated distance (fourth column) and percentage difference (fifth column). SD: Standard Deviation, μ: average, RMSE: Root Mean Square Error

ID point	Measured distance (m)	Measured distance without GCPs (m)	Difference (m)	Percentage difference (%)
2016–2017	3.70	3.79	0.085	2.31
2016–2024	6.27	6.19	−0.081	1.29
2017–2018	1.95	1.95	0.003	0.17
2017–2023	6.75	6.76	0.012	0.18
2018–2019	0.67	0.68	0.009	1.40
2018–2021	1.70	1.68	−0.017	1.03
2018–2022	3.48	3.49	0.006	0.18
2019–2022	3.57	3.59	0.018	0.50
2020–2021	0.86	0.86	−0.007	0.78
2021–2022	2.28	2.30	0.023	1.00
2023–2024	3.79	3.77	−0.021	0.54
2016–2017	3.70	3.79	0.085	2.31
2016–2024	6.27	6.19	−0.081	1.29
SD			**0.05**	
μ			**0.03**	
RMSE			**0.05**	

Table 6. Euclidean distance between point A and point B of structure 5, calculated using the coordinates: measured (second column) and estimated from the reconstruction of the 3D model without Ground Control Points (third column). Difference between the measured distance and the estimated distance (fourth column) and percentage difference (fifth column). SD: Standard Deviation, μ: average, RMSE: Root Mean Square Error

ID point	Measured distance (m)	Measured distance without GCPs (m)	Difference (m)	Percentage difference (%)
2016–2017	3.70	3.79	0.066	1.78
2016–2024	6.27	6.19	−0.156	2.50
2017–2018	1.95	1.95	−0.002	0.09
2017–2023	6.75	6.76	−0.228	3.38
2018–2019	0.67	0.68	0.011	1.58
2018–2021	1.70	1.68	−0.017	1.01
2018–2022	3.48	3.49	−0.058	1.67
2019–2022	3.57	3.59	−0.065	1.81
2020–2021	0.86	0.86	0.010	1.21
2021–2022	2.28	2.30	−0.027	1.21
2023–2024	3.79	3.77	−0.200	5.27
SD			**0.09**	
μ			**− 0.06**	
RMSE			**0.011**	

Table 7. Euclidean distance between point A and point B of structure 5, calculated using the coordinates: measured (second column) and estimated from the reconstruction of the 3D model with target and without Ground Control Points (third column). After the simulation of a damage. Difference between the measured distance and the estimated distance (fourth column) and percentage difference (fifth column). SD: Standard Deviation, μ: average, RMSE: Root Mean Square Error

ID point	Measured distance (m)	Measured distance without GCPs (m)	Difference (m)	Percentage difference (%)
2016–2017	3.70	3.82	0.119	3.22
2016–2024	6.27	6.22	−0.051	0.81
2017–2018	1.95	1.96	0.007	0.35
2017–2023	6.75	6.79	0.037	0.55
2018–2019	0.67	0.68	0.006	0.89
2018–2021	1.70			
2018–2022	3.48	3.50	0.019	0.55
2019–2022	3.57	3.60	0.032	0.89
2020–2021	0.86			
2021–2022	2.28			
2023–2024	3.79	3.83	0.035	0.93
SD			**0.05**	
μ			**− 0.03**	
RMSE			**0.05**	

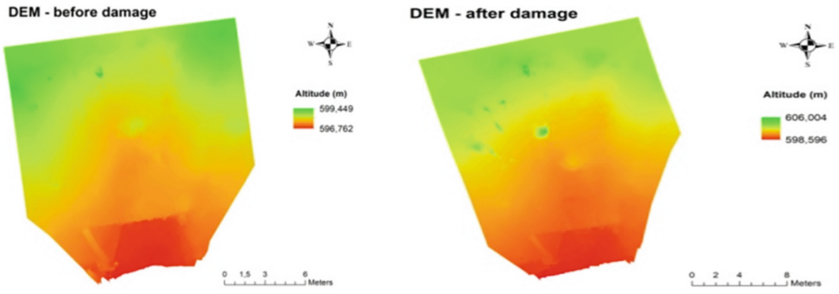

Fig. 12. Digital elevation models: (a) before the damage, (b) after the damage.

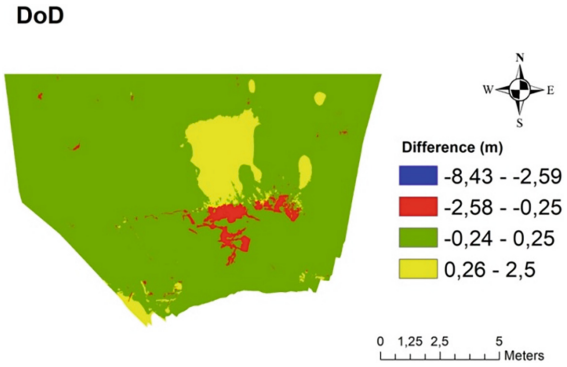

Fig. 13. DoD between the digital elevation model before the damage and the digital elevation model after the damage.

4 Conclusions

The paper is focused on the investigation of small structures in forestry or in mountain areas. Indeed, the paper is aimed to identify a procedure for monitoring the structures for erosion control and slope stabilization, often located in remote locations, without the involvement of professional engineers on the site in order to optimize the use of human high skilled resources. Subsequently, also the quantification of the conditions were conducted. 14 The experiment showed that the methodology is suitable for reaching the objectives of the research. The monitoring of these structures on the territory involves citizens, previously identified and appropriately guided, organizing a "citizen science" program, which is defined as "the collection and analysis of data related to the natural world by an audience that takes part in a collaborative project with professional scientists". The "citizen scientists", using a precise protocol, are a form of active citizenship that allows the development of large-scale monitoring, gathering a considerable amount of data with reduced costs compared to the use of "professionals". The processing does not require such long time of the operator and the images of one or more structures can be processed in about hour. The evaluation phase of any failures, clearly highlighted by the DoD, requires a few minutes for a skilled Forest engineer. In case of doubts, the direct inspection on the field becomes indispensable. As mentioned above, this technique is not proposed for infrastructural constructions, such as bridges or dams. On the contrary, It is well applicable to constructions for which the risk is little or the exposed value is punctually limited or the vulnerability is limited. These constructions are usually poorly monitored, although their failures or lack of maintenance increase the hydrogeology instability of the territory. A quantitative measurement system, such as the one tested, albeit inaccurate, is much more reliable than qualitative assessments based on the memory of the constructions and situations seen years before. The precision of the measurements is not a fundamental parameter in this case; on the contrary, the accuracy that allows the comparison with previous conditions is essential. It was shown that the proposed methodology achieved decimetric accuracy, sufficient in the forest environment. The successive step consists in the development of an App

suitable to disable the zoom and the special effects (like the HDR option), stop the steps and click with sounds, activate the GPS, control the vertical position of the camera, etc., during the acquisition phase. This technique would lead the creation of a 3D database of constructions, largely spread overall the territory, which would progressively be enriched, allowing the planned and orderly management of the thousands of small widespread structures, destined for oblivion.

Acknowledgement. This study was financed by the I.Z.S.Me/C.I.R.AM "Campania trasparente".

References

1. ISTAT annuario statistico italiano 2017, pp. 5–55. ISBN 978-88-458-1933-9. https://www.istat.it/it/files/2017/12/Asi-2017.pdf. Accessed 20 Mar 2019
2. Varnes, D.J.: Landslide hazard zonation: a review of principles and practice (1984). ISBN 92-3-101895-7. https://unesdoc.unesco.org/ark:/48223/pf0000063038
3. Angelats, E., Parés, M.E., Kumar, P.: Feasibility of smartphone based photogrammetric point clouds for the generation of accessibility maps. In: 2018 ISPRS TC II Mid-term Symposium "Towards Photogrammetry 2020". The International Archives of the Photogrammetry, Remote Sensing and Spatial Information Sciences, vol. XLII-2, Riva del Garda, Italy, 4–7 June 2018
4. Caradonna, G., Tarantino, E., Scaioni, M., Figorito, B.: Multi-image 3D reconstruction: a photogrammetric and structure from motion comparative analysis. In: Gervasi, O., et al. (eds.) ICCSA 2018, Part V. LNCS, vol. 10964, pp. 305–316. Springer, Cham (2018). https://doi.org/10.1007/978-3-319-95174-4_25
5. Nocerino, E., Poiesi, F., Remondino, F., Van Gool, L.: Point clouds from smartphones. GIM Int. **32**(3), 18–21 (2018)
6. Masiero, A., Fissore, F., Pirotti, F., Guarnieri, A., Vettore, A.: Toward the use of smartphones for mobile mapping. Geo-Spatial Inf. Sci. **19**(3), 210–221 (2016). https://doi.org/10.1080/10095020.2016.1234684
7. Di grazia, F., Cantelli, L., Fabbri, S., Grumiero, B.: Citizen – photographers help environmental monitoring thanks to a photogrammetric approach, Geophysical Research Abstracts, vol. 20, EGU2018-18099, 2018 EGU General Assembly 2018 (2018)
8. Triglia, A., Iadanza, C., Bussettini, M., Lastoria, B.: Dissesto idrogeologico in Italia: pericolosità ed indicatori di rischio – Edizione 2018. Ispra, Rapporti 287/2018 (2018)
9. Micheletti, N., Chandler, J.H., Lane, S.N.: Investigating the geomorphological potential of freely available and accessible structure-from-motion photogrammetry using a smartphone. Earth Surf. Process. Landf. **40**, 473–486 (2015)
10. Schönberger, J.L., Frahm, J.M.: Structure-from-motion revisited. In: IEEE Conference on Computer Vision and Pattern Recognition, pp. 4104–4113 (2016)
11. Nocerino, E., et al.: 3D reconstruction with a collaborative approach based on smartphones and a cloud-based server. In: 2017 5th International Workshop LowCost 3D – Sensors, Algorithms, Applications. The International Archives of the Photogrammetry, Remote Sensing and Spatial Information Sciences, vol. XLII-2/W8, Hamburg, Germany, 28–29 November 2017

12. Capolupo, A., Pindozzi, S., Okello, C., Fiorentino, N., Boccia, L.: Photogrammetry for environmental monitoring: the use of drones and hydrological models for detection of soil contaminated by copper. Sci. Total Environ. **514**, 298–306 (2015). https://doi.org/10.1016/j.scitotenv.2015.01.109. ISSN: 0048-9697
13. Capolupo, A., Pindozzi, S., Okello, C., Boccia, L.: Indirect field technology for detecting areas object of illegal spills harmful to human health: application of drones, photogrammetry and hydrological models. Geospatial Health **8**, 699–707 (2014). https://doi.org/10.4081/gh.2014.298. ISSN: 1970-7096
14. Capolupo, A., Cervelli, E., Pindozzi, S., Boccia, L.: Assessing volumetric and geomorphologic changes of terraces in Amalfi Coast using photogrammetric technique. In: International Conference AIIA, Bari, Italy, 5–8 July 2017
15. Capolupo, A., Kooistra, L., Boccia, L.: A novel approach for detecting agricultural terraced landscapes from historical and contemporaneous photogrammetric aerial photos. Int. J. Appl. Earth Obs. Geoinf. **73**, 800–810 (2018)